Scheme I

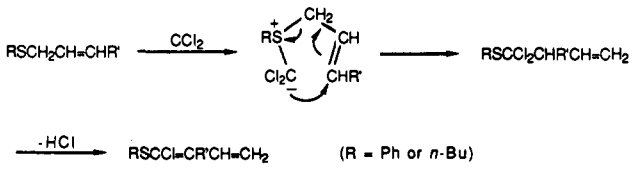

Table I. Kinetics of Ylide Formation and Disappearance[a]

carbene	sulfide	ylide	$10^{-9}k_f$ (M^{-1} s^{-1})[b]	$10^{-6}K_d$ (s^{-1})[c]
PhCCl	**2a**	**3a**	2.3 ± 0.1	12.5 ± 0.5[d]
PhCCl	**2b**	**3b**	4.9 ± 0.2	10 ± 1
PhCCl	**2c**	**3c**[e]	1.8 ± 0.1	5.2 ± 0.3
PhCF	**2a**	**4a**	1.8 ± 0.2	1.7 ± 0.1
PhCF	**2b**	**4b**	4.8 ± 0.5	4.3 ± 0.2
PhCF	**2c**	**4c**	2.1 ± 0.2	2.4 ± 0.1

[a] By LFP[4] in pentane or isooctane solution at 20 °C. [b] Bimolecular rate constant for carbene/sulfide ylide formation, determined in competition with pyridine ylide formation,[3] monitored at 480 nm, [pyridine] = 8×10^{-4} M. [c] First-order rate constant for ylide decay, monitored at 310 nm. [d] An identical rate constant was obtained by monitoring ylide decay at 420 nm. [e] See also structure **7**.

sulfides **2a-c** are all determined in this way; they are collected in Table I.

The decay and rearrangement of ylides **3** and **4** were also examined. Consider, as illustrative, ylide **3a** from PhCCl and sulfide **2a**. LFP generation of PhCCl in 0.011 M **2a** gave ylide **3a**, λ_{max} 310 and 420 nm. The latter absorbance exhibited growth-decay kinetics, consistent with the formation and rearrangement (see below) of **3a**. At 310 nm, we observed non-first-order decay, with the complexity caused by the quenching of PhCCl (formed within the laser pulse[6]) superimposed on the transient absorbance of ylide **3a**. However, at high [sulfide], the PhCCl was quenched so rapidly that *only* the first-order decays of the ylide absorptions were seen at either 310 or 420 nm.[11] Moreover, kinetic analysis furnished identical rate constants, $k_d = (1.2 \pm 0.1) \times 10^7$ s^{-1}, for the decay of **3a** at either wavelength. Importantly, k_d is *independent* of [sulfide] (0.23-0.54 M), so that the rate constant does indeed reflect the first-order disappearance of the ylide. LFP rate constants for the decay of *S*-ylides **3a-c** and **4a-c** (from PhCF) are all similarly determined at [**2a-c**] = 0.09-0.54 M; values of k_d appear in Table I.

The products of these carbene/allyl sulfide reactions were most readily studied with the more volatile methyl allyl sulfides, **2b** and **2c**, which could be more easily removed after reaction than sulfide **2a**.[12] Thus, steady-state irradiation (200-W, focused Osram XE UV lamp, $\lambda > 340$ nm) of phenylchlorodiazirine ($A_{372} = 1.5$) in 0.20 M **2b**-pentane at 20 °C gave >80%[13] of (*E*)- and (*Z*)-1-phenyl-1-(methylthio)-1,3-butadiene (**5**). The structure assignments derive from NMR[14] and GC-MS data (M^+ are *m/e* 176, both isomers). The parallel reaction of PhCF with **2b** also led to *Z*/*E*-**5** in 90% yield. A similar reaction of PhCCl with γ,γ-

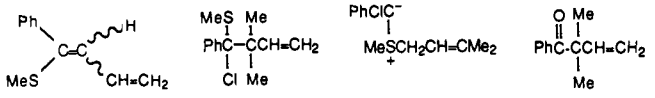

5 **6** **7** (= **3c**) **8**

dimethylallyl methyl sulfide (**2c**) gave a near quantitative mixture of **6**, the [2,3] sigmatropic rearrangement product of the initially formed ylide **3c** (**7**), and ketone **8**, the hydrolysis product of **6**.

(11) We calculate that the pseudo-first-order formation of ylide **3a** at [**2a**] = 0.23 M would be $0.23 \times k_f = 0.23 \times 2.3 \times 10^9 = 5.3 \times 10^8$ s^{-1}, more than 10 times faster than the observed decay of **3a**.

(12) LFP absorbances and kinetic phenomena were entirely analogous for the reactions of PhCCl or PhCF with all three substrates, **2a-c**.

(13) In the presence of excess of K_2CO_3 to neutralize liberated HCl, the yield of **5** exceeded 95%. The isomer ratio was 4:1-7:1 by GC or NMR, respectively.

(14) Major isomer: (200 MHz, δ, $CDCl_3$) 2.22 (s, 3 H, SMe), 4.90-5.22 (m, 2 H, $=CH_2$), 6.15-6.40 (m, 2 H, =CHCH=), 7.34 ("s", 5 H, Ph). The minor isomer (~14%) had δ 1.99 (SMe).

Product characterization was again based on NMR[15] and GC-MS data (M^+ analysis). Attempted purification of **6** on silica gel led to its complete conversion to **8**. The reaction of PhCF with sulfide **2c** followed a course analogous to that of PhCCl.

Clearly, PhCCl and PhCF react with allylic sulfides in a manner parallel to that of CCl_2 (Scheme I).[1] We observe sigmatropic rearrangement of **7** to **6** in the reaction of PhCCl with **2c** and, most importantly, LFP permits us to visualize the formation and decay of the *S*-ylide intermediates in this and related reactions. Table I reveals that, with each substrate, $k_f > 10^9$ M^{-1} s^{-1}. Obviously, the S atom is a voracious carbene trap, far superior to the vinyl groups of these allylic sulfides. Mono- to trisubstituted alkenes react with PhCCl or PhCF with $k \simeq (0.9\text{-}1.3) \times 10^8$ M^{-1} s^{-1},[16] so that we would not expect cyclopropanation to effectively compete with ylide formation from substrates **2**, nor have we observed any cyclopropane products.

The ylides derived from PhCCl (**3a-c**) decay 2-7 times faster than the corresponding ylides (**4a-c**) formed from PhCF (Table I), possibly because enhanced inductive stabilization by F (vs Cl) at the ylides' carbanionic centers slows down the [2,3] rearrangements of the F-substituted ylides. We also observe a modest 2-fold deceleration in the decay of ylides derived from substrate **2c** vs those formed from **2b**. This may be ascribed to the increased steric hindrance to rearrangement offered by the γ-methyl substituents of **2c**.

The present direct observational studies lend strong support to the product-based mechanistic proposals of Parham (Scheme I).[1] The LFP methodology can also be applied to assess solvent effects and activation parameters for these and related carbene ylide reactions.

Acknowledgment. We are grateful to the National Science Foundation for financial support.

(15) ^1H NMR data of **6** (δ, $CDCl_3$): 1.22, 1.24 (2s, 6 H, Me_2C), 1.97 (s, 3 H, SMe), 4.9-5.1 (m, 2 H, $=CH_2$), 6.05-6.20 (m, 1 H, CH=), 7.2-7.4 + 7.7-7.8 (m's, Ph). ^1H NMR data of **8** (δ, $CDCl_3$): 1.40 (s, 6 H, Me_2C), 5.17-5.27 (m, 2 H, $=CH_2$), 6.11-6.26 (m, 1 H, CH=), 7.3-7.5 + 7.8-7.9 (m's, 5 H, Ph); IR (**8**) 1670 cm^{-1} (C=O); M^+, 174.

(16) Moss, R. A.; Turro, N. J. In *Kinetics and Spectroscopy of Carbenes and Biradicals*; Platz, M. S., Ed.; Plenum: New York, 1990; pp 213 f.

Stepwise Transannular Bond Formation between the Bridgehead Atoms in $ZP(MeNCH_2CH_2)_3N$ Systems

J.-S. Tang, M. A. H. Laramay, V. Young, S. Ringrose, R. A. Jacobson, and J. G. Verkade*

Department of Chemistry
Iowa State University
Ames, Iowa 50011
Received January 13, 1992

We have recently described the extraordinary Lewis basicity of the phosphorus in **1** for protons to produce the unexpectedly weak conjugate acid **2**.[1-7] The transannulation process that

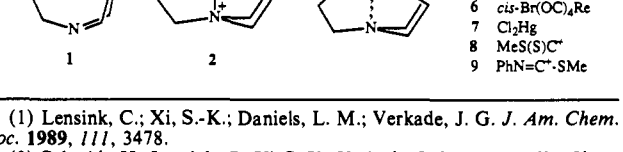

1 **2**

	Z
3	*trans*-$Cl_2Pt(1)$[6]
4	S[6]
5	S_2C[6]
6	*cis*-$Br(OC)_4Re$
7	Cl_2Hg
8	MeS(S)C⁺
9	PhN=C⁺-SMe

(1) Lensink, C.; Xi, S.-K.; Daniels, L. M.; Verkade, J. G. *J. Am. Chem. Soc.* **1989**, *111*, 3478.

(2) Schmidt, H.; Lensink, C.; Xi, S.-K.; Verkade, J. G. *Anorg. Allg. Chem.* **1989**, *578*, 75.

(3) Schmidt, H.; Xi, S.-K.; Lensink, C.; Verkade, J. G. *Phosphorus, Sulfur Silicon* **1990**, *49/50*, 163.

(4) Laramay, M. A. H.; Verkade, J. G. *J. Am. Chem. Soc.* **1990**, *112*, 9421.

(5) Laramay, M. A. H.; Verkade, J. G. *Z. Anorg. Allg. Chem.* **1991**, *605*, 163.

(6) Xi, S. K.; Schmidt, H.; Lensink, C.; Kim, S.; Wintergrass, D.; Daniels, L. M.; Jacobson, R. A.; Verkade, J. G. *Inorg. Chem.* **1990**, *29*, 2214.

0002-7863/92/1514-3129$03.00/0

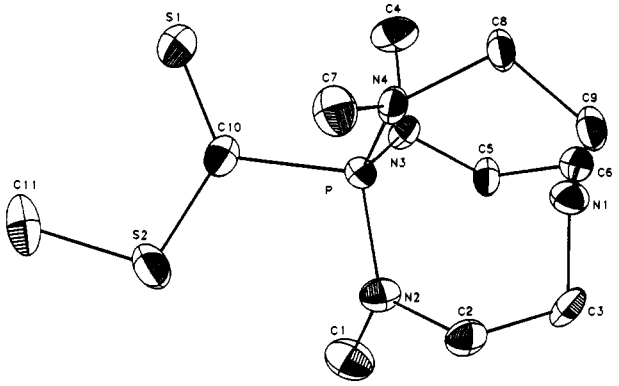

Figure 1. ORTEP drawing for **8** with ellipsoids drawn at the 50% probability level.

accompanies protonation of **1** to give **2** can be viewed as a model of S_N2 formation of a five-coordinate intermediate, with the unusual feature that the nucleophilic atom is forced to invert by virtue of its bridgehead position in the bicyclic structure **1**. It could be expected that exocyclic electrophiles binding to the phosphorus of **1** would be of two kinds, namely, those that cause transannulation and those that do not. However, as we report here, a progression of intermediate P–N_{ax} distances and N_{eq}–P–N_{eq} angles (determined by X-ray means) is observed in **3–9**, marking in a stepwise manner the S_N2 process as a function of the Lewis acidity of the Z substituent.

The new compounds **6–9** are synthesized[8] according to reactions 1–4. Because the ORTEP drawings of **6–9** are similar[9] and those

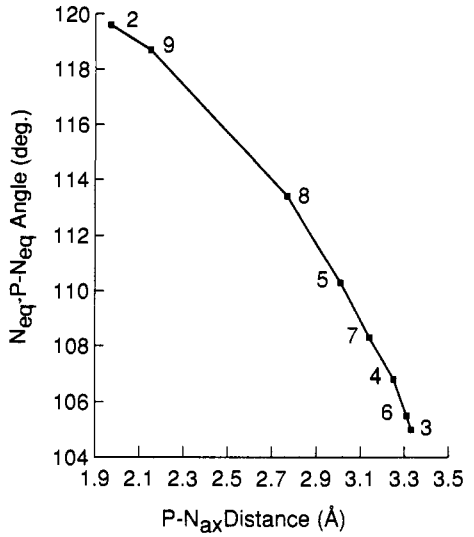

Figure 2. Plot of P–N_{ax} distances (which decrease in the order 3.33, 3.307, 3.250, 3.143, 3.008, 2.771, 2.190, 1.967 Å) against N_{eq}–P–N_{eq} angles (which correspondingly increase in the order 104.5, 105.5, 106.8, 108.3, 110.3, 113.4, 118.6, 119.6°) in $ZP(MeNCH_2CH_2)_3N$ systems **2–9**.

for **2**[1] and **3–5**[6] have been published, only the ORTEP drawing for **8** is shown in Figure 1.

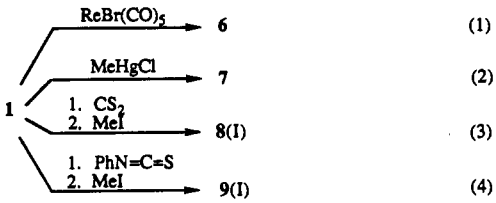

A plot of P–N_{ax} distance versus the N_{eq}–P–N_{eq} angle in Figure 2 reveals a decrease in the P–N_{ax} distance from a value close to the sum of the van der Waals radii (3.34 Å)[10] in **3** (3.33 Å) to a bonded value of 1.967 Å in **2**. Although there is a clearly visible and consistent curvature of this plot, the deviation from linearity (r^2 = 0.98) is relatively small. The nearly monotonic response of the N_{eq}–P–N_{eq} angle to transannulation could arise from a lower reorganization energy associated with phosphorus rehybridization than for other atoms in the bridges tethering the phosphorus to N_{ax}.[11] The only related study we were able to find in the literature concerns a group of eleven Cd(II) thiolate and dithiophosphate structures.[12] Here the response of the S_{eq}–Cd–S_{eq} angle to the approaching nucleophile in the Y–CdS_3···Y′ moiety (Y, Y′ = I, S, or O) was roughly linear (r^2 = 0.88), with no obvious curvature. The roughness of the plot for the Cd(II) complex data must in part be associated with the variation of the nucleophilic species, which in our system is consistently a tertiary nitrogen.

The stepwise establishment of the P–N_{ax} bond depicted in Figure 2 may reflect increasing strain and decreasing entropy associated with the formation of the three five-membered rings in **2**, which counterbalance the electron-withdrawing power of the Z substituent. We have not seen evidence for reaction 5, however, wherein ring strain would not be a factor. Thus only HN^+Et_3

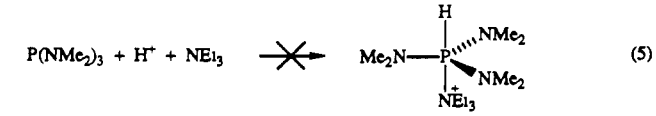

is observed to form. Reaction 5 (wherein after electrophilic attack of the proton two molecules condense to one) probably requires

(7) Verkade, J. G. US Patent 5,051,533, Sept 24, 1991.

(8) A solution of 0.818 g (3.79 mmol) of **1**[1] in 10 mL of THF was added dropwise to a suspension of 1.54 g (3.79 mmol) of $Re(CO)_5Br$ in 20 mL of THF. After 16 h the solvent was removed under vacuum and the residue dissolved in 15 mL of CH_2Cl_2. Slow evaporation gave light yellow single crystals of **6**: 81.8% yield; NMR ^1H, ^{13}C, ^{31}P. Anal. ($C_{10}H_{18}O_4BrN_3PRe$) C, H, N. A solution of 0.324 g (1.50 mmol) of **1**[1] in 10 mL of THF was added dropwise to a solution of 0.377 g (1.50 mmol) of MeHgCl in 15 mL of THF. After 5 min, the supernatant was decanted and the white precipitate of **7** was washed with 2 × 10 mL portions of THF: 98.3% yield; NMR ^1H, ^{13}C, ^{31}P. Anal. ($C_{18}H_{42}Cl_2HgN_3P_2$) C, H, N: calcd 30.7, 6.01, 15.9; found 29.7, 6.13, 15.9. Crystals for X-ray diffraction were grown from CH_2Cl_2 solution. To 0.12 g (0.41 mmol) of **5**[2] was added 1.88 g (13.2 mmol) of MeI. After the exothermic reaction subsided, the residual red solid was dissolved in a minimum of MeCN and the solution stirred for 2 min at room temperature. Evaporation of the volatiles under vacuum gave spectroscopically pure **8**(I) in qualitative yield: NMR ^1H, ^{13}C, ^{31}P; FAB (MeCN) 307.1066 (M^+ of **8**). Anal. ($C_{11}H_{24}IN_4PS_2$) C, H, N. Single crystals of **8** were grown from MeCN at −25 °C. To 0.14 g (0.42 mmol) dissolved in 3 mL of Et_2O was added 0.087 g (0.64 mmol) of PhNCO. After stirring for 5 min, the greenish-yellow solid was collected by filtration, washed with 5 mL of Et_2O, and dried under vacuum. To 0.073 g (2.9 mmol) of this adduct in 1 mL of CH_3CN was added 0.2 mL of MeI. After 30 min of stirring, the volatiles were removed to give **9**(I) quantitatively: MS (FAB, MeCN) 366.3211 (M^+ of **9**, base peak); NMR ^1H, ^{13}C, ^{31}P. Anal. ($C_{17}H_{29}N_5PS$) C, H, N: calcd 41.35, 5.93, 14.19; found 40.82, 5.88, 13.78. Crystals for X-ray diffraction were grown from MeCN at −20 °C.

(9) Crystal data for **6**: orthorhombic crystals, space group *Pbca*: a = 16.291 (2) Å, b = 15.269 (5) Å, c = 15.018 (6) Å, V = 3736 (3) Å^3, D_{calcd} = 2.112 g/cm^3, Z = 8, anisotropic least-squares refinement (Mo Kα radiation, μ(Mo Kα) = 90.0 cm^{-1}, 2416 observed reflections, R = 0.028, R_w = 0.035, diffractometer = Enraf-Nonius CAD4, temperature = −50 °C. Crystal data for **7**: orthorhombic crystals, space group $Pca2_1$; a = 15.557 (6) Å, b = 9.508 (7) Å, c = 18.218 (6) Å, V = 2695 (4) Å, D_{calcd} = 1.753 g/cm^3, Z = 4, anisotropic least-squares refinement (Mo Kα radiation, μ(Mo Kα) = 60.49 cm^{-1}, 2743 observed reflections, R = 0.028, R_w = 0.033, diffractometer = Rigaku AFC6R, temperature = 25 °C). Crystal data for **8**: orthorhombic crystals, space group $P2_12_12_1$; a = 9.975 (5) Å, b = 11.436 (3) Å, c = 14.722 (5) Å, V = 1679 (2) Å^3, D_{calcd} = 1.718 g/cm^3, Z = 4 anisotropic least-squares refinement (Mo Kα radiation, μ(Mo Kα) = 22.6 cm^{-1}, 1629 observed reflections, R = 0.034, R_w = 0.061, diffractometer = Enraf-Nonius CAD4, temperature = −50 °C). Crystal data for **9**: orthorhombic crystals, space group $Pca2_1$, a = 16.786 (3) Å, b = 10.756 (2) Å, c = 24.328 (4) Å, V = 4392 (2) Å^3, D_{calcd} = 1.492 g/cm^3, Z = 8, anisotropic least-squares refinement (Mo Kα radiation, μ(Mo Kα) = 16.5 cm^{-1}, 3024 observed reflections, R = 0.053, R_w = 0.078, diffractometer = Enraf-Nonius CAD4, temperature = 20 °C).

(10) Bondi, A. *J. Phys. Chem.* **1964**, *68*, 441.

(11) A referee has kindly pointed out that a plot of the cosine of the N_{eq}–P–Z angle versus the P–N_{ax} bond length is remarkably linear (r^2 = 1.00).

(12) Bürgi, H. B. *Inorg. Chem.* **1973**, *12*, 2321.

a larger decrease in entropy than transannulation, which is intramolecular. Another factor possibly favoring P–N_{ax} interaction when **1** is electrophilically attacked is the already nearly planar configuration of N_{ax} in **3** (and very probably in **1**) even though the P and N_{ax} atoms are separated by the sum of the van der Waals radii. The planarity of bridgehead nitrogens in bicyclics of this type is apparently due to van der Waals interactions among the CH_2 hydrogens.[6,13]

Acknowledgment. We are grateful to the donors of the Petroleum Research Fund, administered by the American Chemical Society, to the National Science Foundation for grant support of this research, and to Johnson Matthey Aesar/Alfa for platinum reagents through their Metals Loan Program.

Supplementary Material Available: NMR data, ORTEP drawings, description of the data collection and structure solution, and tables of positional and isotropic thermal parameters, bond distances, and angles for **6–9** (53 pages); listing of observed and calculated structure factors for **6–9** (53 pages). Ordering information is given on any current masthead page.

(13) Wang, A. H. J.; Missavage, R. J.; Byrn, J. R.; Paul, I. A. *J. Am. Chem. Soc.* **1972**, *94*, 7100.

Effects of Inter- and Intramolecular Hydrogen Bonding upon the Structure and Photoisomerization of 3-(2-Pyridyl)propenamides

Frederick D. Lewis,* Charlotte L. Stern, and Beth A. Yoon

Department of Chemistry, Northwestern University
Evanston, Illinois 60208-3113

Received September 17, 1991
Revised Manuscript Received January 2, 1992

Intramolecular hydrogen bonding can exert a pronounced effect upon both the thermal[1-5] and photochemical[6-8] equilibria of configurational isomers. For example, the *Z* isomers of enols, enamines, and enamides capable of forming 6-membered intramolecular hydrogen bonds (eq 1) are more stable than their *E* isomers in nonpolar solvents. Disruption of the intramolecular

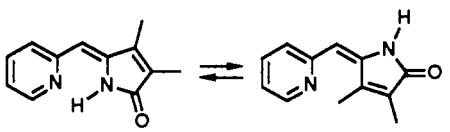

(1)

hydrogen bond by the use of hydrogen bond acceptor solvents such as pyridine or methyl sulfoxide can shift this equilibrium in the direction of the *E* isomer. Photoisomerization of the *Z* isomers of some enols and enamines is reported to yield the *E* isomers, which revert thermally to the *Z* isomers or, in the case of the enols, tautomerize to the corresponding β-dicarbonyl compound, with rates that are subject to acid and base catalysis.[4,5] The *Z* isomers

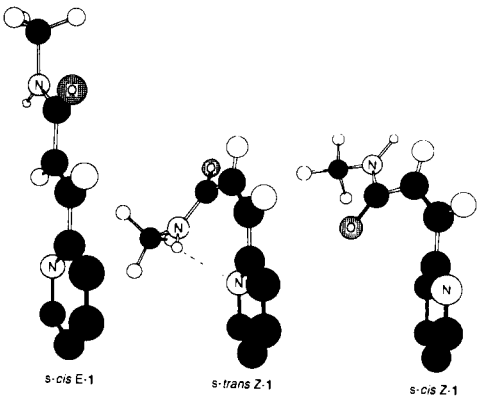

Figure 1. Energy-minimized structures for the low-energy conformers of (*E*)- and (*Z*)-*N*-methyl-3-(2-pyridyl)propenamide. A broken line indicates an intramolecular hydrogen bond.

of α-pyridyl pyrrolinones are reported to be resistant to thermal or photoisomerization in nonpolar solvents, but undergo photoisomerization in alcohol or acidic solvents, which are presumed to disrupt the intramolecular hydrogen bond (eq 1).[6] While less common, there are also examples of molecules in which 7-membered intramolecular hydrogen bonds influence configurational equilibria.[7,8] We report here preliminary results of our investigation of the effects of intra- and intermolecular hydrogen bonding upon the conformation and photochemical behavior of the isomeric *N*-methyl-3-(2-pyridyl)propenamides (*E*- and *Z*-**1**, Figure 1) in solution and in the solid state.

Both *E*- and *Z*-**1** are crystalline solids which are unchanged by prolonged irradiation in the solid state or by heating at their melting points. The molecular packing modes for *E*- and *Z*-**1** (Figure 2) are similar to that for *N*-methylcinnamamide[9] in that chains of molecules are hydrogen bonded via a glide plane.[10] *E*-**1** exists in the s-cis enone conformation and is nearly planar in the solid state, having pyridyl–vinyl and vinyl–amide dihedral angles of 6.2° and 2.2°, respectively. The corresponding dihedral angles for *Z*-**1** are 6.7° and 70.1°. The vinyl–amide dihedral angle is much larger than those previously reported for conjugated amides[9] and presumably is necessary to minimize intermolecular contacts between the chains of (intermolecularly) hydrogen-bonded molecules.

Analysis of the IR and ^1H NMR data for *E*-**1** indicates that its solution conformation is similar to that in the solid state (planar s-cis).[11] The N–H chemical shifts for *E*-**1** in deuteriochloroform and methyl sulfoxide are δ 5.71 and 8.25, respectively, and N–H irradiation results in large NOEs for the α-vinyl hydrogens, but not for the aromatic hydrogens, in both solvents (36.6% and 11.8%, respectively). In contrast, the spectral data for *Z*-**1** are indicative of intramolecular hydrogen bonding in dichloromethane, but not in methyl sulfoxide solution. The N–H chemical shifts for *Z*-**1** in deuteriochloroform and methyl sulfoxide are δ 11.25 and 9.3, respectively. N–H irradiation in deuteriochloroform solution results in a small NOE for the α-vinyl hydrogen (0.9%) and a large NOE for the aromatic hydrogen adjacent to nitrogen (6.3%), whereas, N–H irradiation in methyl sulfoxide solution results in a large NOE for the α-vinyl hydrogen (8.3%) and a small NOE for the aromatic hydrogen adjacent to nitrogen (1.8%). These

(1) Sandström, J. *Top. Stereochem.* **1983**, *14*, 83.
(2) Grande, K. D.; Rosenfeld, S. M. *J. Org. Chem.* **1980**, *45*, 1626.
(3) (a) McMullen, C. H.; Stirling, C. J. M. *J. Chem. Soc. B* **1966**, 1217. (b) Herbig, K.; Huisgen, R.; Huber, H. *Chem. Ber.* **1966**, *99*, 2546.
(4) Henning, H.-G.; Bandlow, M.; Jedrych, Y.; Berlinghoff, R. *J. Prakt. Chem.* **1978**, *320*, 945.
(5) (a) Veierov, D.; Bercovici, T.; Mazur, Y.; Fischer, E. *J. Org. Chem.* **1978**, *43*, 2006. (b) Markov, P.; Petkov, I.; Jeglova, D. *J. Photochem.* **1978**, *8*, 277.
(6) (a) Lightner, D. A.; Park, Y.-T. *J. Heterocycl. Chem.* **1977**, *14*, 415. (b) Falk, H.; Neufingerl, F. *Monatsh. Chem.* **1979**, *110*, 1243.
(7) Eenkhoorn, J. A.; de Silva, S. O.; Snieckus, V. *Can. J. Chem.* **1972**, *51*, 792.
(8) Lewis, F. D.; Howard, D. K.; Oxman, J. D.; Upthagrove, A. L.; Quillen, S. L. *J. Am. Chem. Soc.* **1986**, *108*, 5964.
(9) Leiserowitz, L.; Tuval, M. *Acta Crystallogr.* **1978**, *B34*, 1230.
(10) *E*-**1**: mp 108–110 °C, orthorhombic; space group *Pbca*, a = 9.370 (3) Å, b = 11.003 (2) Å, c = 16.906 Å, V = 1743 (1) Å^3, Z = 8, μ_{calcd} = 0.78 cm^{-1}, ρ_{calcd} = 1.236 g/cm^3; 2192 unique reflections, R = 0.045, R_w = 0.044. *Z*-**1**: mp 72–74 °C; monoclinic; space group $P2_1/c$, a = 10.838 (2) Å, b = 8.712 (2) Å, c = 9.849 (4) A, V = 838.6 (5) Å^3, Z = 4, μ_{calcd} = 0.81 cm^{-1}, ρ_{calcd} = 1.284 g/cm^3; 1826 unique reflections, R = 0.038, R_w = 0.049. An Enraf-Nonius CAD-4 with Mo Kα was used.
(11) *E*-**1**: IR (CCl_4) ν_{N-H} 3450, $\nu_{C=O}$ 1675 cm^{-1}; ^1H NMR ($CDCl_3$) δ 2.96 (d, 3 H), 5.71 (br s, 1 H), 6.97 (d, J = 15.2 Hz, 1 H), 7.25 (t, 1 H), 7.37 (d, 1 H), 7.62 (d, J = 15.2 Hz, 1 H), 7.70 (t, 1 H), 8.62 (d, 1 H). *Z*-**1**: IR (CCl_4) ν_{N-H} 3220, $\nu_{C=O}$ 1655 cm^{-1}; ^1H NMR ($CDCl_3$) δ 2.92 (d, 3 H), 6.16 (d, J = 13.6, 1 H), 6.65 (d, J = 13.6, 1 H), 7.30 (t, 1 H), 7.39 (d, 1 H), 7.79 (m, 1 H), 8.64 (d, 1 H), 11.25 (br s, 1 H).

0002-7863/92/1514-3131$03.00/0